

Thermal production of cold “hot dark matter” around eV

Wen Yin¹

¹*Department of Physics, Tohoku University, Sendai, Miyagi 980-8578, Japan*

A very simple production mechanism of feebly interacting dark matter (DM) that rarely annihilates is thermal production, which predicts the DM mass around eV. This has been widely known as the hot DM scenario. Despite there are several observational hints from background lights suggesting a DM in this mass range, the hot DM scenario has been considered strongly in tension with the structure formation of our Universe because the free-streaming length of the DM produced from thermal reactions was thought to be too long. In this paper, I show that the previous conclusions are not always true depending on the reaction for bosonic DM because of the Bose-enhanced reaction at very low momentum. By using the simple $1 \leftrightarrow 2$ decay/inverse decay process to produce the DM, I demonstrate that the eV range bosonic DM can be thermally produced *coldly* from a hot plasma by performing a model-independent analysis applicable to axion, hidden photon, and other bosonic DM candidates. Therefore, the bosonic DM in the eV mass range may still be special and theoretically well-motivated.

I. INTRODUCTION

The origin of the dark matter (DM) of our Universe has been one of the leading mysteries of particle theory, cosmology, and astronomy for around a century [1]. A few decades ago, thermally produced feebly-interacting DM in the eV mass range was popularly considered, with a leading candidate of the standard model (SM) neutrino (see, e.g., [2]). Indeed, if the feebly-interacting DM once reaches the thermal equilibrium with the thermal bath in the early Universe, the number density of the DM is around that of the photon relic, and the matter-radiation equality, which is known to be around eV temperature, happens at the cosmic temperature around the DM mass. Then the DM mass is predicted around eV. This scenario is well known as the hot DM, which has been considered highly in tension with the structure formation. To be consistent, we need an entropy dilution making DM heavier than a few keV [3, 4]. Moreover, if the DM is a fermion, the Pauli exclusion principle for the DM in galaxies, i.e., the Tremaine-Gunn bound, excludes the mass below ~ 100 eV [5–7]. If the DM is not fully thermalized in the early Universe, e.g., it is produced from a freeze-in mechanism [8], the free-streaming bound still restricts the mass above several keV and excludes the eV mass range [9, 10]. In any case, DM interacting with thermal plasma naïvely acquires momentum around the cosmic temperature, and if the DM is lighter than a keV, the free-streaming length will be too long. It seems that any DM from thermal production with eV mass range is a no-go. On the other hand, recently, there have been hints from the observations of anisotropic cosmic infrared background and TeV gamma-ray spectrum, independently suggesting an axion-like particle (ALP) DM around the eV mass range [11–14] (see also [15–17]).¹ In

the future, there will be various experiments confirming the eV range DM, like the direct detection [22], indirect detection [23], line-intensity mapping [24] (see also some experiments for a generic ALP including this mass range, e.g., solar axion helioscope [25–28] and photon collider [29]). In this paper, I study if the aforementioned no-go theorem for the eV range DM is true. I will show by using a concrete example that the *cold* eV-range bosonic DM can be produced via the thermal interaction with hot plasma by taking into account the Bose-enhancement effect.

As we mentioned, the DM, much lighter than keV, is very likely to be a bosonic one due to the Tremaine-Gunn bound. A known successful scenario that predicts the eV DM is the ALP miracle scenario [30, 31], where the ALP DM is also the inflaton, driving the cosmic inflation. The potential of the ALP is assumed to have an upside-down symmetry, via which the mass, as well as the self-couplings, of the ALP in the vacuum, is related to that during the hilltop inflation. The DM is a remnant of inflaton from a predicted incomplete reheating. Interestingly, the eV mass range is predicted from the conditions for explaining the DM abundance, and the cosmic-microwave background normalization and spectral index for the power spectrum of the scalar density perturbation.²

In this paper, we study another simple production mechanism, predicting the eV mass range: the thermal production that was thought to be excluded in the early studies. I show by considering a two-body decay/inverse decay process,

$$\chi_1 \leftrightarrow \chi_2 \phi \quad (1)$$

¹ In contrast, the anisotropic cosmic infrared background data and the TeV gamma-ray spectrum suggest that the LORRI excess [18] cannot be simply explained by the decay of cold DM [19, 20] (See also [14, 21]).

² Alternatively, there are also various simple DM production mechanisms in standard cosmology that are consistent (but not predict) the eV mass range, like the DM production via inflationary fluctuation [32–36], the light DM production via inflaton decay [37, 38], for ALP with modified potentials [39–41].

of a thermal distributed mother particle, χ_1 , with a mass, $M_1 (\ll T)$, into two daughter particles, χ_2 and ϕ , including a light bosonic particle, ϕ , has a burst population era of the low-momentum mode $p_\phi^{\text{burst}} \sim M_1^2/T$ of ϕ . Here, T is the cosmic temperature at which χ_1 is thermalized. The burst production of ϕ is triggered by the reaction in a timescale $\Delta t_{\text{ignition}} \sim \left(\frac{T^3}{M_1^3} \Gamma_{\chi_1 \rightarrow \chi_2 \phi}^{\text{rest}} \right)^{-1}$ with $\Gamma_{\chi_1 \rightarrow \chi_2 \phi}^{\text{rest}}$ being the proper decay rate of $\chi_1 \rightarrow \chi_2 \phi$. Immediately, the Bose-enhanced production of ϕ populates the momentum modes around p_ϕ^{burst} until the ϕ number density reaches about the number density of χ_1 . Thus low momentum modes of ϕ are produced with a number density around T^3 . In the expanding Universe with the Hubble parameter, H , the condition for this to happen is $\Delta t_{\text{ignition}}^{-1} \gg H$. The momentum of the cold component of ϕ redshifts to be below p_ϕ^{burst} which blue shifts in time. If the usual thermalization rate of χ_2 or ϕ , $\Delta t_{\text{decay}}^{-1} \sim \Gamma_{\chi_1 \rightarrow \chi_2 \phi}^{\text{rest}} M_1/T$, is smaller than H at the burst production, it cannot interact with χ_1, χ_2 anymore through Eq. (1) due to kinematics, and the burst-produced ϕ free-streams until it becomes non-relativistic. Thus if the mass of ϕ is around eV, we get the cold component abundance of ϕ consistent with the measured DM abundance. Since the condition mostly relies on kinematics and statistics, this mechanism easily applies to produce generic bosonic DM, such as axion, hidden photon, and CP-even scalar (a candidate is CP-even ALP [42–44] with dark sector PQ fermions [42]), etc.

The main difference from the previous approaches of freeze-in or thermal production of heavier DM is that I use the unintegrated Boltzmann equation for the evolution of the distribution functions of ϕ and χ_2 by including Bose-enhancement and Pauli-blocking effect as well as the mother particle mass effect. The important assumption is that χ_2, ϕ are both not thermalized when the burst production happens since I focus on light DM, which is typically considered to have a feeble interaction.

The rest of this paper is organized as follows. In the next Sec.II, I will review the Boltzmann equation. In Sec.III, I use a simplified setup neglecting the expansion of the Universe to explain analytically and numerically my mechanism, the burst production of ϕ . In Sec.IV, I will remove several assumptions made in Sec.III, and apply the mechanism to the DM production. I also discuss the conditions that the mechanism is not spoiled by other effects in more generic setups. The last section Sec.V is devoted to discussion and conclusions, in which I will also comment on the application of the mechanism to produce the DM around keV.

II. BOLTZMANN EQUATION

Let us study the production of ϕ via (1) by employing the standard (unintegrated) Boltzmann equation in

expanding Universe (see e.g. [45]),

$$\frac{\partial f_i[p_i, t]}{\partial t} - p_i H \frac{\partial f_i[p_i, t]}{\partial p_i} = C^i[p_i, t], \quad (2)$$

with $i = \chi_1, \chi_2, \phi$ and C^i being the collision term of i ; f_i is the distribution function of i ; $H = \dot{a}/a$ is the Hubble parameter with a being the scale factor; As aforementioned, I do not specify whether ϕ is a vector or a scalar field (or a more generic field with integer spins) but I only assume that ϕ is a boson while $\chi_{1,2}$ may be either fermions or bosons; I assumed the rotational invariance for the equations, and $p_i = |\vec{p}_i|$.

The collision term for, e.g., $i = \phi$ of the $1 \leftrightarrow 2$ process (1) has the form of

$$C^\phi = \frac{1}{2E_\phi g_\phi} \sum \int d\Pi_{\chi_1} d\Pi_{\chi_2} (2\pi)^4 \delta^4(p_{\chi_1} - p_\phi - p_{\chi_2}) \times |\mathcal{M}_{\chi_1 \rightarrow \chi_2 \phi}|^2 \times S(f_{\chi_1}[p_{\chi_1}], f_{\chi_2}[p_{\chi_2}], f_\phi[p_\phi]). \quad (3)$$

with g_i being the internal degrees of freedom including spins, $\mathcal{M}_{\chi_1 \rightarrow \chi_2 \phi}$ the amplitude, $d\Pi_i = \frac{d^3 p_i}{2E_i (2\pi)^3}$ is phase space integral, the sum is performed over all internal degrees of freedom of the initial and final states,

$$S \equiv f_{\chi_1}[p_{\chi_1}](1 \pm f_{\chi_2}[p_{\chi_2}])(1 + f_\phi[p_\phi]) - (1 \pm f_{\chi_1}[p_{\chi_1}])f_\phi[p_\phi]f_{\chi_2}[p_{\chi_2}] = \{f_{\chi_1}(p_{\chi_1})(\pm f_{\chi_2}(p_{\chi_2}) + f_\phi(p_\phi) + 1) - f_{\chi_2}(p_{\chi_2})f_\phi(p_\phi)\} \quad (4)$$

includes the Bose-enhancement and Pauli-exclusion effects. $+$ and $-$ correspond to the cases that $\chi_{1,2}$ are bosons and fermions, respectively.

a. Simplified form with only (1) reaction In this paper, I treat the reaction by Eq. (1) seriously and make some approximations for the other possible reactions. By using the comoving momentum $\hat{p}_i = p_i a$, the Boltzmann equation with collision term (3) reduces to the simplified form

$$\frac{d\hat{f}_\phi[\hat{p}_\phi]}{dt} = \frac{g_{\chi_1}}{g_\phi} \int_{\hat{p}_{\chi_1}^-}^{\hat{p}_{\chi_1}^+} d\hat{p}_{\chi_1} \frac{\hat{p}_{\chi_1}^2}{2\pi^2} \hat{f}_{\chi_1}(\hat{p}_{\chi_1}) \frac{\partial \Gamma_{\chi_1 \rightarrow \chi_2 \phi}^{\text{rest}}}{\gamma \partial \hat{p}_\phi} \frac{S[\hat{f}_i]}{\hat{f}_{\chi_1}(\hat{p}_{\chi_1})}. \quad (6)$$

Here $\hat{p}_{\chi_1}^\pm$ and $d\Gamma_{\chi_1 \rightarrow \chi_2 \phi}^{\text{rest}}/d\hat{p}_\phi$ depend on the kinematics, which will be explained later, $\gamma = E_{\chi_1}/M_1$ (without a hat) the Lorentz factor, and $\hat{f}_i(\hat{p}_i) \equiv f_i(p_i)$. This equation can be understood by multiplying $d\hat{p}_\phi$ on both sides. Then the number density of ϕ in the momentum range $\hat{p}_\phi \sim \hat{p}_\phi + d\hat{p}_\phi$ is produced by the decays minus inverse decays of χ_1 in the whole kinematically-allowed phase space. The reaction rate is accompanied by the Lorentz factor, and the Bose-enhancement and Pauli-blocking factors, S/\hat{f}_{χ_1} , which also includes the inverse decay effect.

The equations for the other particles can be similarly

obtained, e.g., for χ_2 , we have

$$\frac{df_{\chi_2}[\hat{p}_{\chi_2}]}{dt} = \frac{g_{\chi_1}}{g_{\chi_2}} \int_{\hat{p}_{\chi_1}^-}^{\hat{p}_{\chi_1}^+} d\hat{p}_{\chi_1} \frac{\hat{p}_{\chi_1}^2}{2\pi^2} f_{\chi_1}(\hat{p}_{\chi_1}) \frac{\partial \Gamma_{\chi_1 \rightarrow \chi_2 \phi}^{\text{rest}}}{\gamma \partial \hat{p}_{\chi_2}} \frac{S[\hat{f}_i]}{f_{\chi_1}(\hat{p}_{\chi_1})} \quad (7)$$

The collision term via (1) conserves the difference of the comoving number density of χ_2 minus that of ϕ ,

$$(n_{\chi_2} - n_{\phi})a^3 = \text{const}, \quad (8)$$

as long as we do not have other fast interactions to change the comoving number of ϕ or χ_2 . We also have $-\frac{d}{dt}(n_{\chi_1}a^3) = \frac{d}{dt}(n_{\phi}a^3) = \frac{d}{dt}(n_{\chi_2}a^3)$ in the case χ_1 does not have other fast interaction than (1).

b. Kinematics To discuss kinematics, let us first estimate the energy distribution in the boosted frame of χ_1 moving along the z-axis with the Lorentz factor $\gamma = E_{\chi_1}/M_1$. The momentum of the injected ϕ , which has the momentum $p_{\phi}^{\text{rest}} = \frac{M_1^2 - M_2^2}{M_1^2} \frac{M_1}{2}$ with an angle θ_{χ_1} to the z-axis in the rest frame, is boosted as well

$$p_{\phi} = (\gamma + \gamma\beta \cos \theta_{\chi_1}) \times \eta \frac{M_1}{2} = \frac{\eta}{2} (E_{\chi_1} + p_{\chi_1} \cos \theta_{\chi_1}) \quad (9)$$

where $\beta = \sqrt{\gamma^2 - 1}/\gamma$. I include the effect of the mass of χ_2 , M_2 , in

$$\eta \equiv \frac{M_1^2 - M_2^2}{M_1^2} \quad (10)$$

for generality and later convenience. However, I neglect the small ϕ mass, m_{ϕ} , which is only taken into account when we estimate the DM energy density in the next section. Note that the lowest value of p_{ϕ} is $\eta M_1^2/4p_{\chi_1}$ when $p_{\chi_1} \gg M_1$, and $\cos \theta_{\chi_1} = -1$, i.e., ϕ is injected backward.

Then I get

$$\frac{\partial \Gamma_{\chi_1 \rightarrow \chi_2 \phi}^{\text{rest}}}{\partial \hat{p}_{\phi}} = \frac{\Gamma_{\chi_1 \rightarrow \chi_2 \phi}^{\text{rest}}}{\eta \hat{p}_{\chi_1}}. \quad (11)$$

Due to the rotational invariance, we do not have any preferred direction in the rest frame. $p_{\chi_1}^{\pm}$ can be obtained from Eq. (9) with $\cos \theta_{\chi_1}$ in the range $[-1, 1]$.

Before ending this section, I would like to note that given $\Gamma_{\chi_1 \rightarrow \chi_2 \phi}^{\text{rest}}$, M_1, η, g_i and statistics, the equations are irrelevant to intrinsic interactions. This is the reason why I did not specify a model by using an explicit Lagrangian so far (for one explicit Lagrangian, see Sec.IV D). In other words, the mechanism explained by the equations in this section should apply to large classes of models in which ϕ is a bosonic particle.

III. A BURST PRODUCTION OF BOSONIC PARTICLE

In this section, I will study the particle production of ϕ carefully by using the Boltzmann equation in flat space

introduced in the previous section. For clarity, I use a simplified setup to describe the mechanism, and I will remove and discuss the simplifications in the next section, where the mechanism is applied to DM production in cosmology. The simplifications are listed as follows,

Flat Universe: I will neglect the expansion of the Universe, i.e., $a = 1$, and I use Eqs. (6) and (7) by removing the hat. I will recover the effects of the expanding Universe in the following section.

Hierarchical timescales of other interactions: I assume for simplicity that χ_1 is in the thermal equilibrium with the Bose-Einstein (Fermi-Dirac) distribution

$$f_{\chi_1} \approx f_{\chi_1}^{\text{eq}} \equiv \left(e^{E_{\chi_1}/T} \mp 1 \right)^{-1}, \quad (12)$$

where $-$ and $+$ are for the bosonic and fermionic $\chi_{1,2}$, respectively. Here and hereafter, I use the superscript “eq” to denote the quantity in the thermal equilibrium. f_{χ_2} , and f_{ϕ} are treated as variables that evolve via Eqs. (6) and (7). This is a realistic condition if the reaction timescale for the other interactions for χ_1 (χ_2, ϕ) is much faster (slower) than the reactions induced by the process (1). The fast reaction is assumed to keep χ_1 always in the thermal equilibrium. I will come back to argue the case this is not satisfied in Sec.IV C.

Initial conditions: The initial conditions are taken as

$$f_{\chi_2, \phi}[p_i] = 0 \quad \text{at} \quad t = t_i \quad (13)$$

for any p_i . I will comment on what happens by other initial conditions at the end of Sec.III D.

Relativistic plasma: I will focus on the case

$$T \gg M_1 \neq 0. \quad (14)$$

In Sec.IV, this assumption is removed in the expansion Universe.

A. First stage: Ignition

Now we are ready to discuss particle production. Let us focus on the mode of $p_{\phi} \ll M_1$. Then we get from Eq. (9),

$$p_{\chi_1}^- \approx \eta \frac{M_1^2}{4p_{\phi}}, \quad p_{\chi_1}^+ = \infty \quad (15)$$

Thus in Eqs. (6) and (7) only the higher momentum modes of χ_1 can produce the lower momentum mode of p_{ϕ} . In particular, by noting that the dominant mode of the thermal distributed χ_1 has $p_{\chi_1} \sim T (\gg M_1)$, $f_{\phi}(p_{\phi})$ (not $f_{\phi}p_{\phi}^2$) with momentum

$$p_{\phi} \sim p_{\phi}^{\text{burst}} \equiv \eta \frac{M_1^2}{2T} \quad (16)$$

is popularly produced. From the energy-momentum conservation with $p_\phi^{\text{burst}} \ll T$,

$$p_{\chi_1}, p_{\chi_2} \sim T \quad (17)$$

in the reaction. This first stage is characterized by conditions close to the initial one,

$$f_\phi[p_\phi \sim p_\phi^{\text{burst}}] \lesssim 1 \text{ and } f_{\chi_2}[p_{\chi_2} \sim T] \ll 1, \quad (18)$$

and the other momentum modes are also suppressed. Let us follow the evolution of $f_\phi[p_\phi \sim p_\phi^{\text{burst}}]$. By noting $S/f_{\chi_1} \simeq 1$, a timescale that $f_\phi(p_\phi \sim p_\phi^{\text{burst}})$ reaches unity is derived from Eqs. (6), (7) and (18) as

$$\Delta t_{\text{ignition}}^{-1} \sim \frac{g_{\chi_1}}{g_\phi} \frac{4T^3}{\eta^3 M_1^3} \Gamma_{\chi_1 \rightarrow \chi_2 \phi}^{\text{rest}}. \quad (19)$$

We note that at this timescale, χ_1 rarely decays because the thermally averaged decay rate is

$$\Delta t_{\text{decay}}^{-1} \sim \Gamma_{\chi_1 \rightarrow \chi_2 \phi}^{\text{rest}} \frac{M_1}{T}. \quad (20)$$

Only a fraction of

$$\frac{\Delta t_{\text{ignition}}}{\Delta t_{\text{decay}}} \sim \frac{g_\phi \eta^3}{g_{\chi_1}} \frac{M_1^4}{4T^4} (\ll 1), \quad (21)$$

of χ_1 decays. Although the slow decay with a small branching fraction of p_ϕ^{burst}/T decays into ϕ with momentum $p_\phi \sim p_\phi^{\text{burst}}$, it can fill the occupation number in the low momenta modes within a short period because of the small phase space volume $\sim g_\phi (p_\phi^{\text{burst}})^3$. At the

end of this stage characterized by $f_\phi(p_\phi \sim p_\phi^{\text{burst}}) \sim 1$, or $t - t_i \sim \Delta t_{\text{ignition}}$ we have a small occupation number for $p_{\phi, \chi} \sim T$, $f_\phi[p_\phi \sim T]$, $f_{\chi_2}[p_{\chi_2} \sim T] \ll 1$, because of (21).

The numerical result³ for this stage is shown in red shaded region in Fig.1, where I plot the solutions in the $[p_\phi/T \text{ vs } f_\phi]$, $[p_\phi/T \text{ vs } (p_\phi/T)^3 f_\phi]$, $[p_{\chi_2}/T \text{ vs } f_{\chi_2}]$ planes in the three panels from top to bottom, with taking $M_1/T = 1/10$, $\eta = 1$, $\Delta t_{\text{ignition}} = \Delta t_{\text{decay}}/2500 \ll \Delta t_{\text{decay}}$, $t_i = 0$, χ_1, χ_2 as Dirac fermions, and ϕ as singlet scalar with $g_{\chi_{1,2}} = 4$, $g_\phi = 1$. In the top panel, the momentum modes around $p_\phi/T \sim \mathcal{O}(0.001) \sim \eta M_1^2/(2T^2)$ grow to unity with $t \sim \Delta t_{\text{ignition}}$. The timescale is much shorter than Δt_{decay} .

B. Second stage: Burst

What happens afterward is a violent production of ϕ . This stage is characterized by

$$f_\phi[p_\phi \sim p_\phi^{\text{burst}}] \gtrsim 1, f_{\chi_2}(p_{\chi_2} \sim T) \ll 1, \quad (22)$$

with which conditions, we have

$$\left. \frac{S}{f_{\chi_1}} \right|_{p_\phi \sim p_\phi^{\text{burst}}} \sim f_\phi[p_\phi]. \quad (23)$$

From Eq. (6), we derive

$$\dot{f}_\phi[p_\phi \sim p_\phi^{\text{burst}}] \sim \frac{g_{\chi_1}}{g_\phi} \frac{4T^3}{\eta^3 M_1^3} \Gamma_{\chi_1 \rightarrow \chi_2 \phi}^{\text{rest}} f_{\chi_1}[p_{\chi_1} \sim T] f_\phi[p_\phi]. \quad (24)$$

By using the time-independent (12), $f_\phi[p_\phi \sim p_\phi^{\text{burst}}]$ has exponential growth, thanks to the Bose enhancement. The growth rate is $\frac{g_{\chi_1}}{g_\phi} \frac{4T^3}{\eta^3 M_1^3} \Gamma_{\chi_1 \rightarrow \chi_2 \phi}^{\text{rest}} f_{\chi_1} \sim \frac{g_{\chi_1}}{g_\phi} \frac{4T^3}{\eta^3 M_1^3} \Gamma_{\chi_1 \rightarrow \chi_2 \phi}^{\text{rest}} \sim \Delta t_{\text{ignition}}^{-1}$ where I used $f_{\chi_1}[p_{\chi_1} \sim T] \sim 1$. Thus we get

$$\log(f_\phi[p_\phi \sim p_\phi^{\text{burst}}]) \sim \frac{t}{\Delta t_{\text{ignition}}}. \quad (25)$$

Therefore a burst production of ϕ in the low momentum modes around p_ϕ^{burst} of ϕ happens in a timescale not too different from $\Delta t_{\text{ignition}}$.

This stage can be found in the blue-shaded region in Fig.1, which is indeed characterized by the exponential growth of $f_\phi(p_\phi \sim M_1^2/T)$. Note that t are changed with an interval $2\Delta t_{\text{ignition}}$ for the plots here (rather than the exponential changes of the time for the plots in the previous stage). The growth rate is indeed $\sim \mathcal{O}(1) \times 1/\Delta t_{\text{ignition}}$.

C. Final stage: Saturation

The second stage is terminated due to the back reaction from the χ_2 particles, which are simultaneously produced via the bosc-enhanced ϕ production. The relevant χ_2 momentum in the reaction $\chi_1(p_{\chi_1} \sim T) \rightarrow \phi(p_\phi \sim p_\phi^{\text{burst}})\chi_2$ is $p_{\chi_2} \sim T$. Although the phase space volume of χ_2 is much larger than that of ϕ modes around $p_\phi \sim p_\phi^{\text{burst}}$, the exponential production of particles makes $f_{\chi_2}(p_{\chi_2} \sim T)$ soon reaches a quasi-equilibrium. The back reaction from χ_2 stops a further burst production of ϕ . This equilibrium can be estimated by using $S \simeq 0$ with $f_\phi(p_\phi \sim p_\phi^{\text{burst}}) \gg 1$, which leads to

$$f_{\chi_2}(p_{\chi_2} \sim T) \simeq f_{\chi_1}(p_{\chi_1} \sim T) \quad (26)$$

With (12), the number density of χ_2 at this stage is

$$n_{\chi_2} \sim g_{\chi_2} \int_{p_{\chi_2} \sim T} \frac{d^3 p_{\chi_2}}{2\pi^2} f_{\chi_2} \sim g_{\chi_2} \frac{T^3}{\pi^2}. \quad (27)$$

From Eq. (8) and Eq. (13) we arrive at

$$n_\phi[p_\phi \sim p_\phi^{\text{burst}}] = n_\phi^{\text{burst}} \sim g_{\chi_2} \frac{T^3}{\pi^2}. \quad (28)$$

This form is similar to that from thermal distribution, $\sim g_\phi T^3/\pi^2$, but it is different because the internal degrees of

³ Throughout the paper, the Boltzmann equation is solved on the lattices of the momenta, $\{\log \hat{p}_\phi, \log \hat{p}_{\chi_2}\}$, in relevant ranges by using **Mathematica**.

freedom, g_{χ_2} , is for χ_2 and, importantly, it is composed of the low momentum modes, $p_\phi \sim p_\phi^{\text{burst}} \ll T$. I also showed that up to the saturation, the time is only passed by a few $\Delta t_{\text{ignition}}$, therefore, we get the timescale for the burst production process to complete within

$$\Delta t_{\text{burst}} \sim \mathcal{O}(1)\Delta t_{\text{ignition}} \quad (29)$$

In the following analytical estimation, I neglect the short duration of the second stage, and I will use $\Delta t_{\text{ignition}}$ to approximate the timescale to reach the final stage.

The stage discussed here is shown by the plots in the blue-shaded region. They overlap strongly because the system reaches a quasi-equilibrium. In addition, we numerically checked that $n_{\chi_2}[> 0.5T] \approx n_\phi[< 0.01T] \approx 0.36T^3$ at $t = 15\Delta t_{\text{ignition}}$. Here, $n_i[> p_{\text{cutoff}}] \equiv g_i \int_{p_{\text{cutoff}}}^\infty \frac{dp_i p_i^2}{2\pi^2} f_i(p_i)$, $n_i[< p_{\text{cutoff}}] \equiv g_i \int_0^{p_{\text{cutoff}}} \frac{dp_i p_i^2}{2\pi^2} f_i(p_i)$. As a consequence, we have confirmed that the thermal reactions can produce ϕ modes around $p_\phi^{\text{burst}} \ll T$ violently until the number density reaches $\sim g_{\chi_2} T^3/\pi^2$.

D. Slow thermalization after burst, and initial condition dependence

In Fig.1, I also displayed the distribution functions with $t \gg t_{\text{ignition}}$ in the dashed lines. In the middle panel, the number density (\propto the areas below the lines) around p_ϕ^{burst} are suppressed. Although in the next section, I will consider the parameter region that the physics at this timescale is seriously changed due to the expansion of the Universe, let us discuss the evolution in the flat Universe for the understanding of the stability of the quasi-equilibrium reached by the final stage of the burst production.

What is happening is the usual thermalization via the decay/inverse decay at the timescale of $t \sim \Delta t_{\text{decay}}$. At this timescale, an $\mathcal{O}(1)$ fraction of plasma of χ_1 of energy $\mathcal{O}(T)$ decays into χ_2 and ϕ with energies of $\mathcal{O}(T/2)$. Thus $f_{\chi_2}(p_{\chi_2} \sim T/2)$ and $f_\phi(p_\phi \sim T/2)$ tend to increase. This process did not reach an equilibrium so far because the burst production does not produce $f_\phi(p_\phi \sim T/2)$. This happens much after the burst production. From the large hierarchy of the timescale (21) with $T \gg M_1$, the inverse decay via the burst process, $\phi(p_\phi \sim p_\phi^{\text{burst}})\chi_2(p_{\chi_2} \sim T) \rightarrow \chi_1(p_{\chi_2} \sim T)$ happens immediately compensating the usual decay, i.e., it decreases $n_\phi(p_\phi \sim p_\phi^{\text{burst}})$ immediately to keep the quasi-equilibrium (26).

The phenomena discussed here can be seen from the dashed lines with $t = \{0.1, 1, 10\}\Delta t_{\text{decay}}$ in Fig. 1. Strictly speaking, the decrease happens from larger p_ϕ which corresponds to larger $M_1^2/p_{\chi_1, \chi_2}$, which corresponds to the faster boosted decay rate, $\Gamma_{\chi_1 \rightarrow \phi \chi_2} M_1/E_{\chi_1}$. With the exponential hierarchy of timescale (21), $f_\phi(p_\phi \sim M_1^2/4p_0 \ll p_\phi^{\text{burst}})$ at the moment $t \sim \Delta t_{\text{decay}}$ has the production due to ignition with a timescale suppressed by the Boltzmann fac-

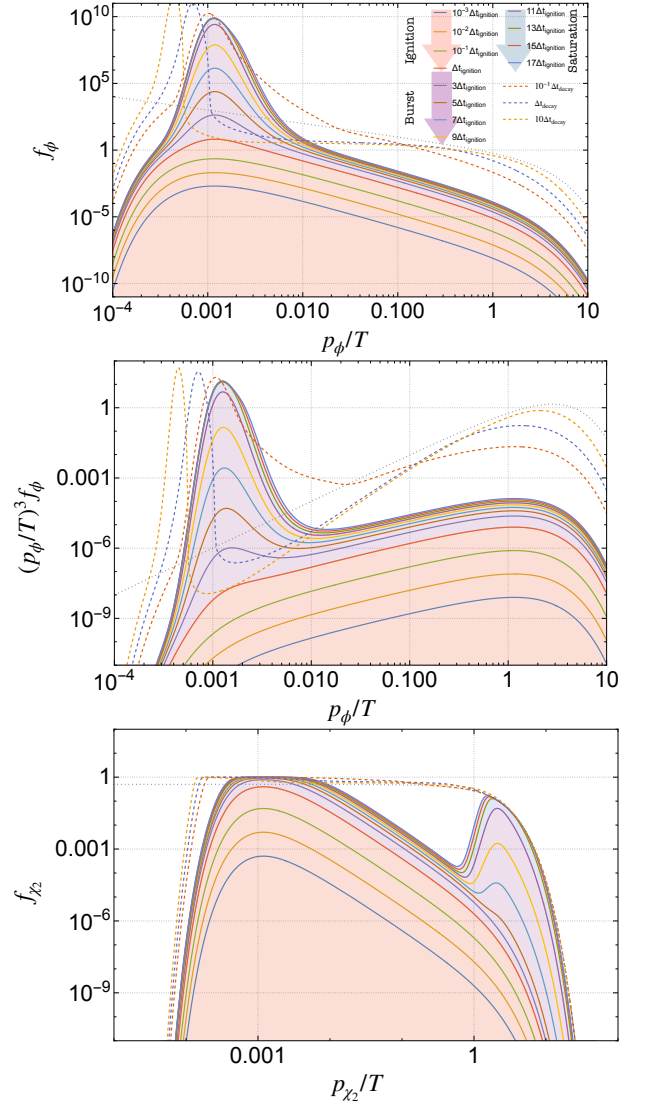


Fig. 1. The numerical solutions of the Boltzmann equation for f_ϕ, f_{χ_2} due to the process Eq. (1) is shown in $f_i[t] - p_i/T$ plane at several t with $t_i = 0$ [top panel]. The Hubble expansion is neglected. We take $M_1/T = 1/10, M_2 = 0$, and $\chi_{1,2}$ to be Dirac fermions with $g_{\chi_{1,2}} = 4$, and ϕ a scalar boson with $g_\phi = 1$. The first stage, the ignition, of the burst production, is shaded in red with four plots for $t = \{10^{-3}, 10^{-2}, 10^{-1}, 1\}\Delta t_{\text{ignition}}$ from bottom to top. The second stage, the burst, corresponds to the purple-shaded regime with four plots of $t = \{3, 5, \dots, 9\}\Delta t_{\text{ignition}}$ from bottom to top. The final stage, saturation, is found in the narrow blue shaded regime with four plots of $t = \{11, 13, \dots, 17\}\Delta t_{\text{ignition}}$. We also show for comparison that the plots with $t = \Delta t_{\text{decay}}$ in dashed lines. Here $\Delta t_{\text{ignition}} = 2500\Delta t_{\text{decay}}$ for the parameter set. In the middle panel, the solutions for $(p_\phi/T)^3 f_\phi$ is also shown. In the bottom panel, we display the solutions in $f_{\chi_2} - p_{\chi_2}/T$ plane in the same setup and the time choices.

tor of $f_{\chi_1}(p_0 \gg T) \sim \exp(-p_0/T)$ in the reaction $f_{\chi_1}(p_0) \rightarrow f_{\chi_2}(p_{\chi_2} \sim p_0)f_\phi(p_\phi \sim M_1^2/4p_0)$. This is the reason why the deeper IR modes are still populated at

$t \sim \Delta t_{\text{decay}}$ in the top and middle panels of Fig. 1. Since the usual thermalization for the deeper UV modes of χ_1, χ_2 , corresponding to the deeper IR modes of ϕ , is suppressed by the Lorentz factor, and Boltzmann suppression $\sim \exp(-2p_0T)$ for $f_{\chi_1}(p_{\chi_1} \sim 2p_0) \rightarrow f_{\chi_2}(p_{\chi_2} \sim p_0), f_{\phi}(p_{\phi} \sim p_0)$ for the usual thermalization process, eliminating the deeper IR mode of ϕ requires a longer timescale than Δt_{decay} .⁴

The lesson we have learned here is that if the usual thermalization of χ_2 at $p_{\chi_2} \sim T$ occurs, the burst-produced ϕ in the IR modes is more-or-less eliminated to maintain the quasi-equilibrium (26). This phenomenon may also happen for the thermalization of χ_2 via the other interactions if they exist.

So far, we have discussed the case that $f_{\chi_2} = f_{\phi} = 0$ as the initial condition. Let me also comment on the numerical results for other initial conditions. I have checked that if we take $f_{\chi_2} \propto f_{\chi_2}^{\text{eq}}$, and $f_{\chi_2} \gtrsim f_{\chi_1}$ initially, the burst ϕ production does not happen. On the contrary, it is also checked that even if ϕ initially has a thermal distribution, we have the burst ϕ production if f_{χ_2} is smaller than f_{χ_1} . They can be well understood by using the quasi-equilibrium (26) and the number conserving feature Eq. (8) of the burst production via (1).

IV. COSMOLOGY OF DM BURST PRODUCTION

Let us apply the burst production mechanism of the bosonic particles studied in the previous Sec.III to produce light DM because the burst-produced particles have $p_{\phi}^{\text{burst}} \ll T$. To discuss the burst production in a more realistic case, let me redefine

$$p_{\phi}^{\text{burst}} \equiv p_{\phi}^{\text{burst}}[T(t)] = \frac{\eta M_1^2}{2T(t)} \quad (30)$$

here and hereafter. It has the same form as the previous section's p_{ϕ}^{burst} , but I introduced the time dependence in $T[t]$ in p_{ϕ}^{burst} , taking account of the Hubble expansion or thermalization of χ_1 . In Sec.IV A, I remove the assumption of the flat Universe and assume the temperature $T[t] \propto a[t]^{-1}$ to show that the burst-produced bosons remain afterward. Then we estimate the DM abundance and discuss some model-independent constraints. Since the production era of the DM is at the highest temperature of $T[t]$ in the regime $T[t] \propto a[t]^{-1}$, this production depends on the UV scenario of the radiation-dominated Universe. In Secs. IV B and IV C, I will consider the scenarios that the DM produced during the reheating and through the thermalization of χ_1 , respectively. In Sec.

IV D I will discuss the model-building for this production mechanism.

A. DM burst production in radiation-dominated Universe

To produce the DM, we need to guarantee that the number density of ϕ via the burst production is not eliminated in the later history of the Universe. This is naturally achieved due to the expansion of the Universe, in which the momenta of free-particle redshifts, while the mass M_i and $\Gamma_{\chi_1 \rightarrow \chi_2 \phi}^{\text{rest}}$ do not. In this section, let us further consider the case in the radiation-dominant Universe by assuming that the burst production timescale or $\Delta t_{\text{ignition}}^{-1}$ is much faster than H , at

$$t = t_i = t_{\text{prod}} \quad (31)$$

which is our initial time for the discussion. The temperature is

$$T[t_{\text{prod}}] = T_{\text{prod}}. \quad (32)$$

I further consider that $\Delta t_{\text{decay}}^{-1}$ is much smaller than the Hubble parameter at $t = t_{\text{prod}}$. Then the burst production occurs because a Hubble time has many $\Delta t_{\text{ignition}}$, and to discuss the burst, we can neglect the Hubble expansion resulting in the essentially same setup as discussed in the previous section. Afterwards the thermal distribution of χ_1 has a time-dependent temperature scaling as

$$T[t] = T_{\text{prod}} \frac{a[t_{\text{prod}}]}{a[t]}. \quad (33)$$

I assumed there is no entropy production or dilution to increase or decrease Ta . Thus the typical momentum for the burst production blueshifts, i.e., $p_{\phi}^{\text{burst}} \propto a$, but particle momentum redshifts, $p_{\phi} \propto a^{-1}$. Within one Hubble time, the momentum of produced light DM before at t_{prod} soon becomes smaller than $p_{\phi}^{\text{burst}}[t]$, i.e.,

$$p_{\phi}^{\text{burst}}(t_{\text{prod}}) \frac{a[t_{\text{prod}}]}{a[t]} < p_{\phi}^{\text{burst}}(t) = p_{\phi}^{\text{burst}}(t_{\text{prod}}) \frac{a[t]}{a[t_{\text{prod}}]}. \quad (34)$$

with $a[t] > a[t_{\text{prod}}]$ due to the redshift and blueshift. Since the production/destruction rate of the modes with $p_{\phi} \ll p_{\phi}^{\text{burst}}$ via Eq. (1) is Boltzmann suppressed by $f_{\chi_1} \sim e^{-\eta M_1^2/(2p_{\phi}T)}$ (see Eq. (6)), the DM production/destruction for the mode produced at $t = t_{\text{prod}}$ will be kept intact later thanks to the expansion of Universe.

The production of modes around $p_{\phi} \sim p_{\phi}^{\text{burst}}[t]$ later is also suppressed since $f_{\chi_2}(p_{\chi_2} \sim T)$ reaches the quasi-equilibrium $f_{\chi_1}(p_{\chi_1} \sim T) \sim f_{\chi_2}(p_{\chi_2} \sim T)$ at the first short moment $t \approx t_{\text{prod}}$. This is because $p_{\chi_1}, p_{\chi_2} \propto a^{-1}, T \propto a^{-1}$ later. In other words, once χ_2 has the number density $\sim g_{\chi_2} T^3/\pi^2$, which is close to the upper bound from the thermal production, Eq. (8) also sets

⁴ With this kind of suppressed IR modes, we can produce heavier DM than eV range, coldly, by explaining the measured DM abundance.

the upper bound of the number density of ϕ . Therefore once $n_\phi \sim n_\phi^{\text{burst}} \sim g_{\chi_2} T_{\text{prod}}^3 / \pi^2$ is fulfilled due to the burst production, the reaction is afterward suppressed. A numerical simulation for a similar setup is shown in Fig. 2 by assuming a phase of reheating followed by the radiation-dominated Universe (see for a detailed explanation of the figure in Sec.IV B). We see the burst-produced component indeed is frozen at a much later time at which the $p_\phi \sim T$ modes are mostly thermalized. This is a very different point from the case in flat Universe Sec.III D.

To sum up, the condition for the burst production to occur in the radiation dominated Universe is

$$\Delta t_{\text{ignition}}^{-1} \gg H \gg \Delta t_{\text{decay}}^{-1} \text{ at } T = T_{\text{prod}} \quad (35)$$

The first inequality is that the Hubble expansion can be neglected compared with the timescale for the burst production. The second inequality is for suppressing the usual thermalization eliminating the burst-produced ϕ . This is because with $\Delta t_{\text{ignition}}^{-1}, \Delta t_{\text{decay}}^{-1} \gg H$, the setup by neglecting the Hubble expansion will be essentially the same as in Sec.III D (with additional interaction for ϕ, χ_2 , the additionally induced thermalization of χ_2 and ϕ should probably be also smaller than the Hubble rate [see Sec.IV C]). If this is satisfied the DM is produced with (28) with $T = T_{\text{prod}}$.

One notices with the assumption $T \propto a^{-1}$ and $H \propto a^{-2}$, the condition (35) is more likely to satisfy in an early time. In other words, the production should be UV scenario dependent. Since in the following subsections, we will focus on some natural scenarios that the discussion here is applicable by properly choosing T_{prod} , let us continue our discussion.

a. DM abundance and the mass range Once the condition (35) is satisfied, later, the ratio of the burst-produced DM number density to plasma entropy density conserves until today. The cold component of the abundance can be estimated from

$$\Omega_\phi = m_\phi \frac{n_\phi^{\text{burst}}}{s} \bigg|_{T=T_{\text{prod}}} \frac{s_0}{\rho_c}. \quad (36)$$

Here ρ_c, s_0 are the present critical density and the entropy density, respectively, and $n_\phi^{\text{burst}} \sim g_{\chi_2} T_{\text{prod}}^3 / \pi^2$ (see Eq. (28)), $s = g_{\star, s} \frac{2\pi^2}{45} T_{\text{prod}}^3$. $g_{\star, s}$ is the relativistic degrees of freedom for entropy, (g_\star will be used as the degrees for energy density). $g_{\star, s}$ should include $(7/8)^f (g_{\chi_1} + g_{\chi_2})$ with $f = 1(0)$ for fermionic (bosonic) $\chi_{1,2}$, because they are relativistic soon after the burst. In the following, I assume that the comoving entropy carried by $\chi_{1,2}$ is released to the lighter SM particles before the neutrino decoupling. In addition, $\chi_{1,2}$ are supposed not to dominate the Universe during the thermal history (no further entropy production other than $\sim g_{\chi_1} T^3, g_{\chi_2} T^3$). By requiring the ϕ abundance Ω_ϕ equal to the measured DM density [1] $\Omega_{\text{DM}} \approx 0.26$, I, therefore, get

$$m_\phi = 50 \text{eV} \frac{4}{g_{\chi_2}} \frac{g_{\star, s}[T_{\text{prod}}]}{100}. \quad (37)$$

Since $g_{\star, s}$ include g_{χ_2} , at the $g_{\chi_2} \rightarrow \infty$ limit, this reduces to the lower bound of the mass of ϕ , while we may also have an upper bound by restricting $g_{\star, s} \lesssim \mathcal{O}(100)$:

$$2 \text{eV} \lesssim m_\phi \lesssim \mathcal{O}(100) \text{eV} \quad (38)$$

is the generic prediction.⁵

b. Constraints from structure formation To have successful structure formation, we need the free-streaming length of the DM to be sufficiently suppressed. The free-streaming length of the cold component can be estimated by using,

$$L_{\text{FS}} = a_0 \int^{t_{\text{eq}}} dt v_\phi[t]. \quad (39)$$

Here v_ϕ is the typical physical velocity of ϕ DM, a_0 is the present scale factor, t_{eq} is the time at matter-radiation equality. By approximating $v_\phi \sim \frac{p_\phi^{\text{burst}}(t_{\text{prod}})a[t_{\text{prod}}]/a}{\sqrt{(p_\phi^{\text{burst}}(t_{\text{prod}})a[t_{\text{prod}}]/a)^2 + m_\phi^2}}$, the bound $L_{\text{FS}} < 0.06 \text{Mpc}$ [3, 4] (see a similar mapping for heavy DM from inflaton decay [46]) leads to

$$\sqrt{\eta} \frac{M_1}{T_{\text{prod}}} \lesssim 0.02 \left(\frac{g_{\star}[T_{\text{prod}}]}{100} \right)^{1/6} \sqrt{\frac{m_\phi}{\text{eV}}}. \quad (40)$$

The required hierarchy is not too large.⁶

c. Suppression of the hot components Strictly speaking, other than the burst-produced component, production of ϕ may occur via the usual decay/inverse decay process. This implies we may have a mixed DM after the decoupling of ϕ from the thermal plasma

$$n_\phi^{\text{tot}}[t] = n_\phi^{\text{burst}}[t] + n_\phi^{\text{th}}[t] \quad (41)$$

where the first term denotes the part from the burst produced component, which is dominated by the momentum mode $p_\phi^{\text{burst}} \sim \eta M_1^2 a[t_{\text{prod}}] / (2T_{\text{prod}} a[t]) \ll T[t]$, while the latter one is from the ordinary thermal production via Eq. (1). We have neglected the latter component so far in discussing the free-streaming length. Indeed, the hot component n_ϕ^{th} of ϕ should be suppressed to be below $\mathcal{O}(1-10)\%$ level depending on the mass range [47]. Indeed in the numerical simulation for Fig. 2, I get $n_\phi^{\text{th}}/n_\phi^{\text{tot}} \equiv \frac{n_\phi[<0.1T]}{n_\phi[<0.1T] + n_\phi[>0.1T]}|_{t=5 \times 10^5 t_R} \sim 30\%$ for $\chi_{1,2}$ being the Dirac fermion case (top panel), and dominant hot components for $\chi_{1,2}$ being singlet scalars (middle panel). They may be in tension with the constraint.

⁵ If there is a large amount of entropy production after the production by, e.g., χ_1, χ_2 dominating the Universe, the DM can be heavier, which is not taken into account here.

⁶ Therefore, I will not discuss the model-dependent issues, e.g., the coherent scattering and the perturbativity of the Boltzmann equation, that are important when the occupation number is very large.

Here let me point out three kinds of parameter regions with suppressed hot DM components.

First, we can suppress the hot DM component by considering $\eta \lesssim 1$, i.e., the mass of χ_2 is non-negligible. The contribution can be analytically estimated by using $n_\phi^{\text{th}} \sim \eta^3 T^3/\pi^2$, because the momentum of ϕ can be at most produced up to ηT (see Eq. (9)). We expect a near thermal distribution at $p_\phi \lesssim \eta T$ while the spectrum is suppressed at $p_\phi \gtrsim \eta T$ compared to the thermal one. For instance, with $\eta = 1/2$, in the bottom panel of Fig. 2, the thermal component is indeed suppressed. We checked $n_\phi^{\text{th}}/n_\phi^{\text{tot}} \sim 3\%$. In this case, p_ϕ^{burst} is also suppressed (see the Figure c.f. Eq. (16)).

The second possibility is to consider the small m_ϕ range by taking $g_{\chi_1}/g_{\star,s}$ large in Eq. (37). The effects have already been seen by comparing the top and middle panels in Fig. 2. If the mass is below 5 – 10 eV with $T_{\text{prod}} \gtrsim 100$ GeV, we can have a successful cold DM scenario together with the hot DM similar to the scenarios [30, 31]. This scenario may be naturally justified if χ_i are charged under some non-abelian group.⁷

The last possibility is that $\Delta t_{\text{decay}}^{-1}$ never becomes faster than H until $T \sim M_1$. This may be considered as the “freeze-in” scenario in which the usual interaction rate with the plasma for ϕ is always smaller than the Hubble expansion. Then the usual thermal production of $f_\phi(p_\phi \sim T)$ is always suppressed, and thus $n_\phi^{\text{th}}/n_\phi^{\text{tot}}$ is suppressed. One numerical example is shown in Fig. 3, where the hot component is suppressed to be $n_\phi^{\text{th}}/n_\phi^{\text{tot}} \sim 5\%$ (See Sec. IV B for detail of the figure).

I also comment that the hot DM bound disfavors the simple scenario $\chi_2 = \phi$. This is because $f_\phi[p_\phi \sim T] = f_{\chi_2}[p_\phi \sim T]$ is also obtained via the burst production (as seen from the middle panel of Fig. 2). Any of the above possibilities may not be useful for this case.

B. DM burst production during reheating

One realistic possibility that the setup for the numerical simulation can apply is the DM production at the end of reheating. Given that χ_1 is always thermalized, the burst production was found to be UV-dependent in the radiation-dominated Universe, which motivates me also to study the behavior during the reheating phase. To be more concrete, let us focus on the case $\Delta t_{\text{ignition}}^{-1}$ is faster than the Hubble expansion rate at the end of

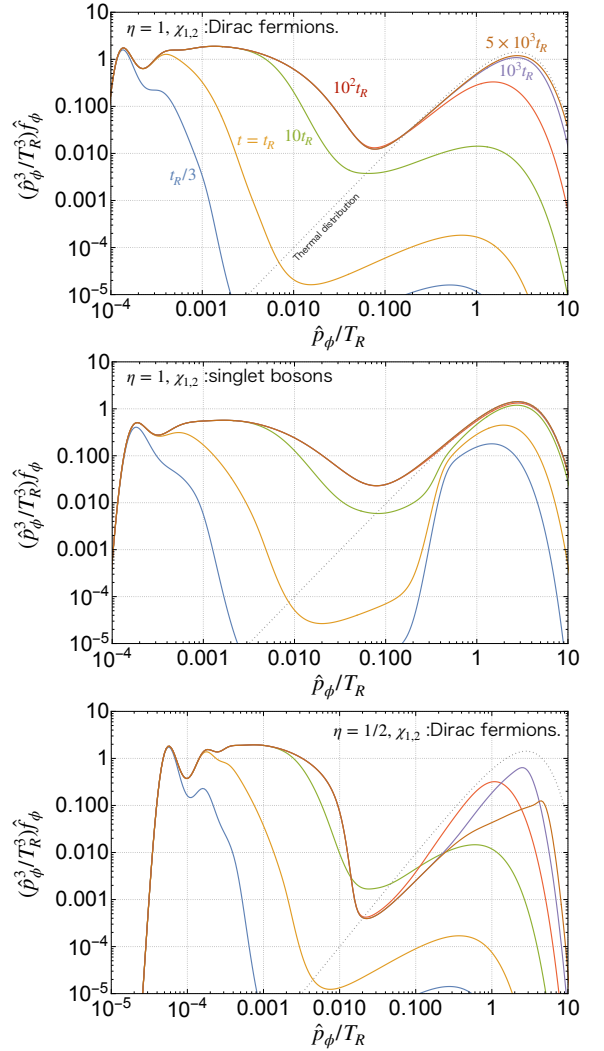


Fig. 2. The numerical simulation of DM distribution function $\hat{p}_\phi^3 T_R^{-3} \hat{f}_\phi$ in expanding Universe by varying \hat{p}_ϕ/T_R with $t = \{1/3, 1, 10, 10^2, 10^3, 5 \times 10^3\} t_R$. The initial cosmic time is $t_i = 1/10 t_R$ at which $\hat{f}_{\chi_2} = \hat{f}_\phi = 0$ is set. $\Gamma_{\chi_1 \rightarrow \chi_2 \phi} = 10^{-3} t_R^{-1}$, $M_1 = T_R/10$. We take $g_{\chi_{1,2}} = 4$ with $\chi_{1,2}$ being fermions in the top panel. The dotted line shows the thermal distribution for ϕ . $\hat{p}_i \equiv p_i a[t]/a_R$. In the middle and bottom panels, cases with $\eta = 1$, and $1/2$ with $g_{\chi_{1,2}} = 1$ and 4 and $\chi_{1,2}$ being singlet scalars and fermions are shown, respectively. Other parameters/variables are the same as in the top panel. In all panels, I consider ϕ as a scalar with $g_\phi = 1$.

reheating $t = t_R$,

$$\Delta t_{\text{ignition}}^{-1}|_{t=t_R} \gg H(t = t_R). \quad (42)$$

$t = t_R$ is defined by $H = \sqrt{\rho_{\text{tot}}/3M_{\text{pl}}^2} = \Gamma_{\text{reh}}$ where Γ_{reh} is the decay rate of inflaton, moduli or other particle that is responsible for reheating, ρ_{tot} the total energy density of the Universe, $M_{\text{pl}} \approx 2.4 \times 10^{18}$ GeV the reduced Planck scale. The cosmic temperature at this moment is defined as $T = T_R$.

⁷ In the scenarios solving the quality problem by using a non-abelian gauge group, multiple PQ Higgs bosons/singlet fermions with similar masses may be predicted [48–51]. Also, the scenario generically predicts fermions/bosons with large internal degrees. There may also be additional neutral bosons in the scenarios enhancing the sphaleron rate for baryogenesis with lower reheating temperature than electroweak scale [52] and the model having QCD axion DM around eV with larger decay constant than the conventional one [53].

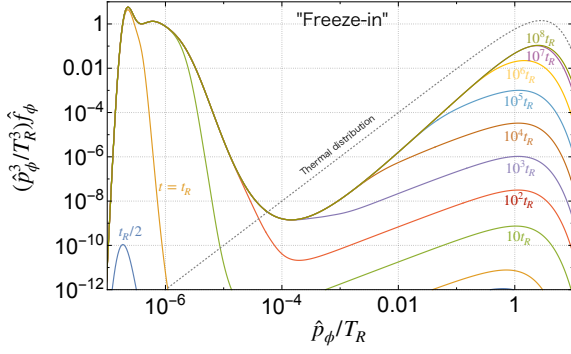


Fig. 3. The numerical simulation for the “freeze-in” scenario that the usual thermalization rate of ϕ is always slower than the Hubble rate. Setups are the same as the top panel in Fig. 2. I take $t_i = 1/3t_R$, $M_1 = T$ at $t = 2.5 \times 10^5 t_R$, at which $\Gamma_{\chi_1 \rightarrow \chi_2 \phi}^{\text{rest}} = 0.01H$. The plots are for $t = \{1/2, 1, 10, 10^2, 10^3, 10^4, 10^5, 10^6, 10^7, 10^8\}t_R$ from bottom to top.

During the reheating, the radiation is continuously produced via $\rho_r \sim \rho_{\text{tot}} \Gamma_{\text{reh}}/H$. As conventionally, I assume the matter-dominated Universe during the reheating, $H \propto a^{-3/2}$, $\rho_{\text{tot}} \propto a^{-3}$, which gradually decays into radiation. Thus $T \propto \rho_r^{1/4} \propto a^{-3/8}$, i.e., the temperature of the plasma due to the reheating decreases slower than a^{-1} . The ignition rate scales as

$$\Delta t_{\text{ignition}}^{-1}|_{t < t_R} \propto T^3 \propto a^{-9/8} \quad (43)$$

which decreases slower than the Hubble rate, i.e., during the reheating, the ignition rate is IR dominant. Given Eq. (42), the burst production rate is still larger than the Hubble rate if we go back in time for a while, during which we have the burst production. Indeed, to satisfy the quasi-equilibrium condition Eq. (26) during the reheating phase, χ_2 is gradually produced through Eq. (1), and $f_{\chi_2}(p_{\chi_2})$ also scales with $T \propto a^{-3/8}$. In the period with the quasi-equilibrium, χ_2 has the comoving number density, $n_{\chi_2}^{\text{quasi-eq.}} a^3 \propto a^{15/8}$. Thus I get

$$\frac{d}{dt} (n_{\chi_2}^{\text{quasi-eq.}} a^3) \propto H a^{15/8} \propto a^{3/8}. \quad (44)$$

This increases in time during the reheating, the largest comoving number density is produced at the last Hubble time in the reheating phase. After the end of the reheating, the momenta on both sides of Eq. (26) scales as a^{-1} , and the production of the comoving number density of χ_2 is suppressed, as discussed in Sec. IV A. From Eq. (8), the ϕ IR modes are also produced gradually and most efficiently at the end of the reheating. Thus, we can choose

$$T_{\text{prod}} \sim T_R \quad (45)$$

as a not-too-bad approximation. The typical momentum of ϕ due to the burst production is then around $\frac{\eta M_1^2}{2T_R} \frac{a[t_R]}{a[t]}$.

I simulate this scenario to get the ϕ spectrum in Fig. 2. I used $a = a_R(t/t_0)^{1/2} \tanh((t/t_0)^{1/6})$ and $T = T_0(a_R/a) \tanh(a/a_R)^{5/8}$, i.e. the reheating ends at $a = a_R \sim a[t_R]$, $t = t_R$, in Eqs. (6), (7), and (12).

I displayed $\frac{p_\phi^2 a^3[t]}{T_R^3 a_R^3} f_\phi$ in expanding Universe by varying $p_\phi a[t]/a_R T_R$ at $t = \{1/3, 1, 10, 10^2, 10^3, 5 \times 10^3\}t_R$ from bottom to top. The initial time is chosen as $t_i = 1/10t_R$ at which $\hat{f}_{\chi_2} = \hat{f}_\phi = 0$ is set. $\Gamma_{\chi_1 \rightarrow \chi_2 \phi} = 10^{-3}t_R^{-1}$, $M_1 = T_R/10$. I take $\eta = 1$, $\chi_{1,2}$ are Dirac fermions (singlet bosons) with $g_{\chi_{1,2}} = 4(1)$ in the top (middle) panel, and take $\eta = 1/2$ for $\chi_{1,2}$ being Dirac fermions with $g_{\chi_{1,2}} = 4$ in the bottom panel. In Fig. 3, the same setup as the top panel of Fig. 2 is plotted, but I take $t_i = 1/3t_R$,⁸ $M_1 = T$ at $t = 2.5 \times 10^5 t_R$, at which $\Gamma_{\chi_1 \rightarrow \chi_2 \phi}^{\text{rest}} = 0.01H$, i.e. the Δt^{decay} is $\mathcal{O}(100)$ times longer than the age of the Universe when χ_1 becomes non-relativistic. The plots are for $t = \{1/2, 1, 10, 10^2, 10^3, 10^4, 10^5, 10^6, 10^7, 10^8\}t_R$ from bottom to top.

We can see in any case that ϕ is burst-produced at the momentum mode $p_\phi^{\text{burst}}(T_R)/T_R = \eta M_1^2/(2T_R^2) \sim \eta \times \mathcal{O}(0.001)$, at the time $t = \mathcal{O}(1)t_R$. Later, the cold component around the comoving momentum $p_\phi^{\text{burst}}(t_R)a[t_R]/a[t]T_R$ is frozen later for exponentially long time.

From the above discussion, it is clear that the DM mass (37) and coldness (40) can be estimated by using Eq. (45).

C. DM burst production during thermalization

One can also consider the DM production during the thermalization of χ_1 . Here, for generality, I use $\Gamma_{\text{th},1}$, $\Gamma_{\text{th},2}$ and $\Gamma_{\text{th},\phi}$, respectively, for denoting the thermalization rate for χ_1, χ_2 and ϕ from some additional reactions than Eq. (1), like the scatterings with other SM particle plasma with temperature $T \propto a^{-1}$. I will neglect $\Gamma_{\text{th},2}$ and $\Gamma_{\text{th},\phi}$ in the main discussion, and I will come back at the end of this subsection. Initially I take $f_{\chi_1, \chi_2, \phi} = 0$, and $\Gamma_{\text{th},1} < H$ at $t = t_i$. Furthermore, I assume the radiation-dominated Universe, and $\Gamma_{\text{th},1}/H \propto a^{q_{\text{th},1}}$ with $q_{\text{th},1}$ being a positive number. For instance, the thermalization via the renormalizable interactions with relativistic particles may have $\Gamma_{\text{th},1} \propto T$

⁸ To reduce the calculation cost, I took a relatively close initial time to t_R for the end of reheating. There is a sharp peak, which should be understood as the burst produced ϕ at $t \sim t_i$ with the initial condition $f_{\phi, \chi_2} = 0$, which seems to be dominant for the number density. This number is expected to be diluted if reheating lasts long, and the spectrum becomes UV insensitive (while the total amount of $n_\phi^{\text{burst}} a^3|_{t \gg t_R}$ does not change much if $n_{\chi_2} \sim g_{\chi_2} T^3/\pi^2$ after the reheating before the thermalization due to Eq. (8)). On the other hand, this $t_i \sim t_R$ simulation will be a not-too-bad assumption by considering some scenarios with a short reheating phase. For instance, the ALP inflation scenarios [54–56] and some scenarios for baryogenesis after the supercooling [57–59] (see also [60, 61]) have this feature.

from dimensional arguments, leading to $q_{\text{th},1} = 1$. With those assumptions, we have a cosmic time $t_{\text{th},1}$ and cosmic temperature $T_{\text{th},1}$ that $\Gamma_{\text{th},1} = H$.

Although a more detailed study of thermalization relies on the momentum-dependent and model-dependent interactions of χ_1 , let us assume that thermalization mainly occurs for the number density with the typical momentum $p_{\chi_1} \sim T$ for simplicity. If $\chi_{1,2}$ are fermions, this should be a good approximation because the reaction that produces IR modes with small phase space volume is soon Pauli-blocked. Thus $f_{\chi_1}(p_{\chi_1} \sim T)$ increases with time with

$$f_{\chi_1}(p_{\chi_1} \sim T) \sim \frac{\Gamma_{\text{th},1}}{H} \text{ with } t \ll t_{\text{th}}. \quad (46)$$

To estimate the ignition rate, let us take account of f_{χ_1} in the integral of Eq. (6), and use

$$\Delta t_{\text{ignition}}^{-1} \equiv \frac{g_{\chi_1}}{g_\phi} \frac{T^3}{4\eta^3 M_1^3} \Gamma_{\chi_1 \rightarrow \chi_2 \phi}^{\text{rest}} \frac{f_{\chi_1}(p_{\chi_1} \sim T)}{f_{\chi_1}^{\text{eq}}(p_{\chi_1} \sim T)} \quad (47)$$

where $\frac{f_{\chi_1}(p_{\chi_1} \sim T)}{f_{\chi_1}^{\text{eq}}(p_{\chi_1} \sim T)}$ was 1 in the previous analysis since we assumed χ_1 in the thermal equilibrium Eq. (12). In particular, we focus on the case that burst production rate is faster than the Hubble rate at the thermalization,⁹

$$\Delta t_{\text{ignition}}^{-1} \gg H \text{ at } t = t_{\text{th},1}. \quad (48)$$

It scales as for $t \ll t_{\text{th},1}$

$$\Delta t_{\text{ignition}}^{-1} \propto a^{-3+q_{\text{th},1}}. \quad (49)$$

This is UV (IR) dominant if $q_{\text{th},1} < 1$ (> 1) during the thermalization. In any case, slightly before $t_{\text{th},1}$, the ignition rate is still faster than the Hubble parameter satisfying Eq. (48).

In the time regime, $(\Delta t_{\text{ignition}})^{-1} \gg H$, during the thermalization of χ_1 Eq. (26) is reached with $f_{\chi_1} < f_{\chi_1}^{\text{eq}}$.¹⁰ Since $n_\phi^{\text{burst}} \sim g_{\chi_2} \int_{p_{\chi_2} \sim T} d^3 p_{\chi_2} f_{\chi_2} \sim g_{\chi_2} \int_{p_{\chi_1} \sim T} d^3 p_{\chi_1} f_{\chi_1} \propto \frac{\Gamma_{\text{th}}}{H} T^3 \propto a^{-3+q_{\text{th},1}}$, the comoving number density of $n_\phi^{\text{burst}} a^3$ increases in time. At $t > t_{\text{th},1}$,

it is frozen out as discussed in Sec.IV A. Therefore the dominant production happens at the cosmic temperature $T = T_{\text{th},1}$ which is the cosmic temperature that χ_1 is fully thermalized, $f_{\chi_1} \approx f_{\chi_1}^{\text{eq}}$. At this moment, we get $f_{\chi_2} \sim f_{\chi_1}^{\text{eq}}$. Thus

$$T_{\text{prod}} \sim T_{\text{th},1}. \quad (50)$$

I numerically checked a similar behavior in the setup more-or-less close to this scenario with a simple modification, Eq. (12) $\rightarrow f_{\chi_1} = \tanh(\Gamma_{\text{th},1}/H) (e^{E_{\chi_1}/T} \mp 1)^{-1}$ with $a \propto t^{1/2}$.

Lastly, I comment on the thermalization rate of $\Gamma_{\text{th},2}$ and $\Gamma_{\text{th},\phi}$. $\Gamma_{\text{th},2}$ for the momentum mode around T should be slower than the H at least at $T = T_{\text{th},1}$ since, otherwise, the $p_{\chi_2} \sim T$ modes of χ_2 reach the equilibrium, and thus the resulting burst-produced ϕ is suppressed (c.f. Eq. (8) is only for the reaction of Eq. (1), and Sec.III D). Similarly, $\Gamma_{\text{th},\phi}$ for the low momentum mode should be smaller than H at the production. In addition, after the burst production, $\Gamma_{\text{th},\phi}$ for the low momentum mode may also be required to be smaller than the Hubble parameter because otherwise, the produced ϕ is washed out. This is a usual assumption for the light DM. The consistency of the argument is checked by introducing the terms $-\Gamma_{\text{th},\phi}(\hat{f}_\phi[\hat{p}_\phi] - \hat{f}_\phi^{\text{eq}}[\hat{p}_\phi])$, and $-\Gamma_{\text{th},2}(\hat{f}_{\chi_2}[\hat{p}_{\chi_2}] - \hat{f}_{\chi_2}^{\text{eq}}[\hat{p}_{\chi_2}])$ in the Boltzmann equations (6) and (7), respectively. That said, I emphasize that the arguments may have exceptions due to the momentum dependence of the reaction and Bose enhancement. A more detailed model-dependent analysis by performing the Boltzmann equation will be desired.

D. Model-building –case of ALP coupled to right-handed neutrinos–

Let me roughly discuss possible models for the burst production of ϕ DM. By assuming that ϕ is an SM gauge singlet, $\chi_{1,2}$ should have the representation for the gauge group. In the case, $\chi_{1,2}$ has a non-trivial representation of the SM gauge group, the requirement $\Gamma_{\text{th},2} \ll H$ can be only satisfied in the high-temperature regime, for instance, $T_R \gtrsim 10^{13-14}$ GeV SU(2) gauge interactions are decoupled (e.g. [62]). In this case, we can use charged heavy beyond SM (BSM) particles to play the roles of χ_1 in the burst production of ϕ . We will not consider this possibility but focus on the case that $\chi_{1,2}$ are also gauge singlets. The theoretical candidates may be the BSM singlet scalars, and fermions in various BSM scenarios (see also the footnote. 7), e.g., some supersymmetric partners, or right-handed neutrinos (RHN), the latter of which I will explain in more detail.

The RHNs may exist to explain the smallness of the active neutrino masses by the seesaw mechanism [63–66] (see also [67] and a UV completion for charge quantization predicting the neutrino mass scale [68]) and to produce baryon asymmetry via leptogenesis [69–73] (see

⁹ If this is not satisfied, but satisfied in the early stage of thermalization, $t \ll t_{\text{th},1}$ when $f_{\chi_1} < f_{\chi_1}^{\text{eq}}$, we will have the suppressed $n_\phi^{\text{burst}} < g_{\chi_2} T_{\text{prod}}^3/\pi^2$ with T_{prod} being the cosmic temperature at $H = \Delta t_{\text{ignition}}^{-1}$. Thus the DM mass to explain the DM abundance is enhanced. This is the case $q_{\text{th},1} < 1$, because $t_{\text{ignition}}^{-1} \propto a^{-3+q_{\text{th},1}}$ decreases faster than $H \propto a^{-2}$ does.

¹⁰ Strictly speaking, when $\Gamma_{\text{th},1}$ is slower than H , that is slower than $\Delta t_{\text{ignition}}^{-1}$, the back reaction to f_{χ_1} due to the interaction (1) exists. It decreases f_{χ_1} at $t < t_{\text{th},1}$ compared to the discussed case neglecting this backreaction. The decrease is in a way satisfying the comoving number conservation $-\Delta(n_{\chi_1} a^3) = \Delta(n_{\chi_2} a^3) = \Delta(n_\phi a^3)$ via Eq. (1). Taking account of this effect should not change our conclusions because, in the end, we will get χ_1 thermalized, with $f_{\chi_2}(p_{\chi_2} \sim T) \sim f_{\chi_1}(p_{\chi_1} \sim T) \sim f_{\chi_1}^{\text{eq}}(p_{\chi_1} \sim T)$. During the whole process Eq. (8) is guaranteed.

also [62, 74, 75] in the effective theory with lepton flavor oscillation). The Lagrangian is given as

$$\mathcal{L}_N = i\bar{N}_i\partial_\mu\gamma^\mu N_i - \left(\frac{1}{2}M_{ij}\bar{N}_i^c N_j + y_{N,i\alpha}\bar{L}_\alpha\tilde{H}\hat{P}_R N_i + \text{h.c.}\right), \quad (51)$$

where L_α is a left-handed lepton field in the chiral representation, \tilde{H} is the Higgs doublet field, $i, (\alpha)$ runs from 1 to n (e, μ, τ), and we take $M_{ij} = M_i\delta_{ij}$ and M_i to be real without loss of generality. I do not restrict to the case $n = 3$ or 2 but take n generic.

The thermalization of the RHN in the mass range of interest can be estimated as

$$\Gamma_{N,i}^{\text{th}} \simeq \gamma_N \sum_{\alpha} |y_{N,i\alpha}|^2 T \quad (52)$$

with $\gamma_N \simeq 0.01$ being the numerical result from Refs. [76, 77] which includes $2 \leftrightarrow 2$ and $1 \leftrightarrow 2$ processes with SM particles as well as the Landau-Pomeranchuk-Migdal effects [78, 79]. By comparing $\Gamma_{N,i}^{\text{th}}$ with the Hubble parameter at the radiation dominated era, $H \simeq \sqrt{g_*\pi^2 T^4/90M_{\text{pl}}^2}$, one obtains the temperature that N is thermalized

$$T_{\text{th},i} \simeq 7 \text{ TeV} \left(\frac{\sum_{\alpha} |y_{N,i\alpha}|^2}{10^{-6}} \right)^2. \quad (53)$$

The right-handed neutrino, N_i , can also couple to the light bosonic DM, especially the ALP, with a derivative coupling like

$$\mathcal{L}_{\text{eff}}^{\text{int}} \supset \sum_{i \geq j} C_{N_i N_j} \frac{\partial_\mu \phi}{2f_\phi} \bar{N}_i \gamma_5 \gamma^\mu N_j. \quad (54)$$

Moving to a mass basis by field redefinitions to remove ϕ in the derivative, we obtain,

$$\mathcal{L}_{\text{mass}} = i \sum_{i \geq j} C_{N_i N_j} (M_i + M_j) \frac{\phi}{2f_\phi} \bar{N}_i^c \gamma_5 N_j. \quad (55)$$

This interaction introduces the decay of

$$N_1 \rightarrow a N_{i \neq 1} \quad (56)$$

where N_1 is the heaviest RHN. The ignition rate can be estimated as

$$(\Delta t_{\text{ignition}})^{-1} \sim \sum_{i \neq 1} C_{N_1, N_i}^2 \frac{T^3}{4\pi f_\phi^2}. \quad (57)$$

After this timescale, the ALP burst production occurs, stimulating all reactions (56) via the Bose enhancement if the ALP couplings in the mass basis are not exponentially small. We can easily find that the ignition rate is faster than the Hubble expansion rate at T if

$$f_\phi \lesssim 2 \times 10^9 \text{ GeV} \sqrt{\sum_{i \neq 1} C_{N_1, N_i}^2} \sqrt{\frac{T}{100 \text{ GeV}}}. \quad (58)$$

From this, for the ALP with $f_\phi \sim 10^{6-8} \text{ GeV}$ that is relevant to EBL hints and future reaches mentioned in the introduction, the process is very efficient. If N_1 has the highest thermalization temperature after reheating,

$$T_R \gg T_{\text{th},1} \gg T_{\text{th},i \neq 1} \quad (\rightarrow \text{Sec.III D}) \quad (59)$$

this becomes the setup of Sec.III D with $T_{\text{prod}} = T_{\text{th},1}$, while if

$$T_{\text{th},1} \gg T_R \gg T_{\text{th},i \neq 1} \quad (\rightarrow \text{Sec.IV B}) \quad (60)$$

it becomes the setup of Sec.IV B with $T_{\text{prod}} = T_R$. In any case, $N_{i \neq 1}$ are gradually thermalized after the burst production via the reaction to all channels $N_1 \rightarrow a N_2, \dots, a N_n$. We can estimate the DM abundance with Eq. (37) by taking $g_{\chi_2} = 2 \times (n-1)$. Via the active-neutrino Yukawa interactions, the comoving entropy carried by RHNs gets back to the SM much after the ϕ burst production.

The hot component of ϕ from the decay and inverse decay can be suppressed with the mild degeneracy of $M_1 \sim M_{i \neq 1}$, which can lead to slightly larger $y_{N,i}$ to explain the neutrino mass via the seesaw mechanism. Also, the hot component can be suppressed by considering relatively large f_ϕ for the suppressed $\Delta t_{\text{decay}}^{-1}$, or simply have DM light as discussed in Sec.IV A.¹¹

Since ALP is usually defined as an axion coupled to a pair of photons, I also check the thermalization of the ALP via the photon coupling. Thermalization rate for the $2 \rightarrow 2$ process involving an ALP and photon, e.g., $e\bar{e} \rightarrow \gamma a$, is roughly estimated $\Gamma_{\text{th}} \sim \alpha^3 T^3 / f_\phi^2$, which is several orders of magnitude smaller than the ignition rate. Here $\alpha \sim 1/128$ is the fine-structure constant.¹² The thermalization does not occur for $T \lesssim T_{\text{th},\phi}^{(\gamma)} \sim 0.3 \text{ TeV} \frac{f_\phi}{10^7 \text{ GeV}}$. As long as this thermalization is inefficient at the burst production period at $T \sim T_{\text{prod}} < T_{\text{th},\phi}^{(\gamma)}$, the cold DM production happens. Even if the thermal relic of ϕ exists at $T = T_{\text{prod}}$ the burst production occurs (see the last part of Sec.III D). Interestingly, the hot component produced initially via the ALP-photon coupling is suppressed with $\eta < 1$ due to the inverse decay $\phi N_{i \neq 1} \rightarrow N_1$ at $T \sim M_1$, as numerically checked in

¹¹ It is straightforward to apply the model to a hidden photon DM whose gauge coupling is not too large. Thanks to the equivalence theorem, we can consider ϕ as the longitudinal mode of the photon with certain UV completions. Model-independently, the ignition rate for N_1 decaying into the longitudinal mode and $N_{i \neq 1}$ does not change. The N_1 decay into the transverse mode is neglected because of the small gauge coupling. However, the discussion in the following, including the thermalization via photon coupling and decays into neutrinos, are only for the ALP.

¹² This may be replaced by the one for SM $SU(2)_L$ or $U(1)_Y$ coupling in the symmetric phase, which decreases the upper bound of T . With only $U(1)_Y$ coupling, the discussion does not change much.

the last panel of Fig.2.¹³ Later, the ALP produced via the burst is kept intact because the dissipation rate via the interactions is suppressed by the tiny momentum as usual [84] (see also another estimation by treating the ALP as an oscillating field [85]).

A prediction of this scenario is that the ALP also decays into active neutrinos. The mass range can be reached by future cosmic neutrino background searches like PTOLEMY [86–88].

V. CONCLUSIONS AND DISCUSSION

In this paper, I have shown that the thermal production of dark matter (DM) with a mass around eV may not result in the DM being as hot as has been considered. The coldness of the produced DM depends on the details of the reaction that produces the DM, given that the TG bound favors the DM as a bosonic field in the mass range of eV. In a very short period, the bosonic DM may be burst-produced in much lower momentum modes than the cosmic temperature due to a Bose enhancement. Since the DM with the burst production naturally has the number density around that of the thermalized mother particles due to the back-reaction, the mass is predicted around eV, the mass range of the conventional hot DM. The cold component of the DM can remain until today if the cosmic expansion makes the burst reaction freeze out. One successful example has been discussed by focusing on the simple $1 \leftrightarrow 2$ decay/inverse decay reaction without adopting the conventional approximations: (1)

all the particles except for the DM are treated in thermal distribution and (2) neglect of the Bose-enhancement and Pauli-blocking factors. The resulting DM abundance predicts the mass in the range of

$$m_{\text{DM}} = \mathcal{O}(1 - 100) \text{ eV}. \quad (61)$$

In summary, I claim that the eV mass range for the DM may still be special, and it should be theoretically well motivated.

So far, I have used the simplest reaction to demonstrate my claim. There may be other examples of the light and cold bosonic DM production from hot plasma, e.g., via generic many to many scatterings, Bremsstrahlung emissions of hidden photons, etc., which are worth further studies.

I also comment that in the whole discussion, I considered the possibility that various timescales have hierarchies, e.g., Eq. (35). Without the hierarchy, we may have less cold DM number and thus heavier DM mass, e.g., a few keV, for the abundance. Some examples were explained in footnotes 4 and 9. The DM in this scenario is colder than that of the usual thermally produced DM with the same mass. Thus the structure formation bounds for the DM can be relaxed.

ACKNOWLEDGMENTS

I thank Brian Batell for useful discussions on Boltzmann equations in another ongoing project. The present work is supported by JSPS KAKENHI Grant Numbers 20H05851, 21K20364, 22K14029, and 22H01215.

-
- [1] N. Aghanim *et al.* (Planck), *Astron. Astrophys.* **641**, A6 (2020), [Erratum: *Astron. Astrophys.* 652, C4 (2021)], arXiv:1807.06209 [astro-ph.CO].
 - [2] C. S. Frenk and S. D. M. White, *Annalen Phys.* **524**, 507 (2012), arXiv:1210.0544 [astro-ph.CO].
 - [3] M. Viel, J. Lesgourgues, M. G. Haehnelt, S. Matarrese, and A. Riotto, *Phys. Rev. D* **71**, 063534 (2005), arXiv:astro-ph/0501562.
 - [4] V. Iršič *et al.*, *Phys. Rev. D* **96**, 023522 (2017), arXiv:1702.01764 [astro-ph.CO].
 - [5] S. Tremaine and J. E. Gunn, *Phys. Rev. Lett.* **42**, 407 (1979).
 - [6] A. Boyarsky, O. Ruchayskiy, and D. Iakubovskiy, *JCAP* **03**, 005 (2009), arXiv:0808.3902 [hep-ph].
 - [7] L. Randall, J. Scholtz, and J. Unwin, *Mon. Not. Roy. Astron. Soc.* **467**, 1515 (2017), arXiv:1611.04590 [astro-ph.GA].
 - [8] L. J. Hall, K. Jedamzik, J. March-Russell, and S. M. West, *JHEP* **03**, 080 (2010), arXiv:0911.1120 [hep-ph].
 - [9] A. Kamada and K. Yanagi, *JCAP* **11**, 029 (2019), arXiv:1907.04558 [hep-ph].
 - [10] F. D’Eramo and A. Lenoci, *JCAP* **10**, 045 (2021), arXiv:2012.01446 [hep-ph].
 - [11] Y. Gong, A. Cooray, K. Mitchell-Wynne, X. Chen, M. Zemcov, and J. Smidt, *Astrophys. J.* **825**, 104 (2016), arXiv:1511.01577 [astro-ph.CO].
 - [12] A. Korochkin, A. Neronov, and D. Semikoz, *JCAP* **03**, 064 (2020), arXiv:1911.13291 [hep-ph].
 - [13] A. Caputo, A. Vittino, N. Fornengo, M. Regis, and M. Taoso, *JCAP* **05**, 046 (2021), arXiv:2012.09179 [astro-ph.CO].
 - [14] J. L. Bernal, A. Caputo, G. Sato-Polito, J. Mirocha, and M. Kamionkowski, (2022), arXiv:2208.13794 [astro-ph.CO].
 - [15] K. Kohri, T. Moroi, and K. Nakayama, *Phys. Lett. B* **772**, 628 (2017), arXiv:1706.04921 [astro-ph.CO].
 - [16] O. E. Kalashev, A. Kusenko, and E. Vitagliano, *Phys. Rev. D* **99**, 023002 (2019), arXiv:1808.05613 [hep-ph].
-
- ¹³ This phenomenon may be also useful for suppressing the hot relics of the axion in the hadronic QCD axion window, an interesting eV range DM candidate [80, 81] (See also [82, 83]) by introducing the BSM particles $\chi_{1,2}$ coupled to QCD axion. Burst production after the freeze out of the axion-hadron interaction can be useful for the axion cold DM production if it can be made consistent with the big-bang nucleosynthesis.

- [17] A. Kashlinsky, R. G. Arendt, F. Atrio-Barandela, N. Cappelluti, A. Ferrara, and G. Hasinger, *Rev. Mod. Phys.* **90**, 025006 (2018), arXiv:1802.07774 [astro-ph.CO].
- [18] T. R. Lauer et al., *Astrophys. J. Lett.* **927**, L8 (2022), arXiv:2202.04273 [astro-ph.GA].
- [19] K. Nakayama and W. Yin, *Phys. Rev. D* **106**, 103505 (2022), arXiv:2205.01079 [hep-ph].
- [20] P. Carenza, G. Lucente, and E. Vitagliano, (2023), arXiv:2301.06560 [hep-ph].
- [21] J. L. Bernal, G. Sato-Polito, and M. Kamionkowski, *Phys. Rev. Lett.* **129**, 231301 (2022), arXiv:2203.11236 [astro-ph.CO].
- [22] M. Baryakhtar, J. Huang, and R. Lasenby, *Phys. Rev. D* **98**, 035006 (2018), arXiv:1803.11455 [hep-ph].
- [23] T. Bessho, Y. Ikeda, and W. Yin, *Phys. Rev. D* **106**, 095025 (2022), arXiv:2208.05975 [hep-ph].
- [24] M. Shirasaki, *Phys. Rev. D* **103**, 103014 (2021), arXiv:2102.00580 [astro-ph.CO].
- [25] I. G. Irastorza et al., *JCAP* **06**, 013 (2011), arXiv:1103.5334 [hep-ex].
- [26] E. Armengaud et al., *JINST* **9**, T05002 (2014), arXiv:1401.3233 [physics.ins-det].
- [27] E. Armengaud et al. (IAXO), *JCAP* **06**, 047 (2019), arXiv:1904.09155 [hep-ph].
- [28] A. Abeln et al. (IAXO), *JHEP* **05**, 137 (2021), arXiv:2010.12076 [physics.ins-det].
- [29] K. Homma, F. Ishibashi, Y. Kirita, and T. Hasada, *Universe* **9**, 20 (2023), arXiv:2212.13012 [hep-ph].
- [30] R. Daido, F. Takahashi, and W. Yin, *JCAP* **05**, 044 (2017), arXiv:1702.03284 [hep-ph].
- [31] R. Daido, F. Takahashi, and W. Yin, *JHEP* **02**, 104 (2018), arXiv:1710.11107 [hep-ph].
- [32] P. W. Graham and A. Scherlis, *Phys. Rev. D* **98**, 035017 (2018), arXiv:1805.07362 [hep-ph].
- [33] F. Takahashi, W. Yin, and A. H. Guth, *Phys. Rev. D* **98**, 015042 (2018), arXiv:1805.08763 [hep-ph].
- [34] S.-Y. Ho, F. Takahashi, and W. Yin, *JHEP* **04**, 149 (2019), arXiv:1901.01240 [hep-ph].
- [35] P. W. Graham, J. Mardon, and S. Rajendran, *Phys. Rev. D* **93**, 103520 (2016), arXiv:1504.02102 [hep-ph].
- [36] Y. Ema, K. Nakayama, and Y. Tang, *JHEP* **07**, 060 (2019), arXiv:1903.10973 [hep-ph].
- [37] T. Moroi and W. Yin, *JHEP* **03**, 301 (2021), arXiv:2011.09475 [hep-ph].
- [38] T. Moroi and W. Yin, *JHEP* **03**, 296 (2021), arXiv:2011.12285 [hep-ph].
- [39] P. Arias, D. Cadamuro, M. Goodsell, J. Jaeckel, J. Redondo, and A. Ringwald, *JCAP* **06**, 013 (2012), arXiv:1201.5902 [hep-ph].
- [40] S. Nakagawa, F. Takahashi, and W. Yin, *JCAP* **05**, 004 (2020), arXiv:2002.12195 [hep-ph].
- [41] D. J. E. Marsh and W. Yin, *JHEP* **01**, 169 (2021), arXiv:1912.08188 [hep-ph].
- [42] K. Sakurai and W. Yin, *JHEP* **04**, 113 (2022), arXiv:2111.03653 [hep-ph].
- [43] K. Sakurai and W. Yin, (2022), arXiv:2204.01739 [hep-ph].
- [44] G. Haghighat, M. Mohammadi Najafabadi, K. Sakurai, and W. Yin, (2022), arXiv:2209.07565 [hep-ph].
- [45] E. W. Kolb and M. S. Turner, *The Early Universe*, Vol. 69 (1990).
- [46] Q. Li, T. Moroi, K. Nakayama, and W. Yin, *JHEP* **09**, 179 (2021), arXiv:2105.13358 [hep-ph].
- [47] R. Diamanti, S. Ando, S. Gariazzo, O. Mena, and C. Weniger, *JCAP* **06**, 008 (2017), arXiv:1701.03128 [astro-ph.CO].
- [48] L. Di Luzio, E. Nardi, and L. Ubaldi, *Phys. Rev. Lett.* **119**, 011801 (2017), arXiv:1704.01122 [hep-ph].
- [49] H.-S. Lee and W. Yin, *Phys. Rev. D* **99**, 015041 (2019), arXiv:1811.04039 [hep-ph].
- [50] M. Ardu, L. Di Luzio, G. Landini, A. Strumia, D. Teresi, and J.-W. Wang, *JHEP* **11**, 090 (2020), arXiv:2007.12663 [hep-ph].
- [51] W. Yin, *JHEP* **10**, 032 (2020), arXiv:2007.13320 [hep-ph].
- [52] J. Jaeckel and W. Yin, *Phys. Rev. D* **107**, 015001 (2023), arXiv:2206.06376 [hep-ph].
- [53] P. Agrawal and K. Howe, *JHEP* **12**, 029 (2018), arXiv:1710.04213 [hep-ph].
- [54] F. Takahashi and W. Yin, *JHEP* **07**, 095 (2019), arXiv:1903.00462 [hep-ph].
- [55] F. Takahashi, M. Yamada, and W. Yin, *JHEP* **01**, 152 (2021), arXiv:2007.10311 [hep-ph].
- [56] F. Takahashi and W. Yin, *JCAP* **10**, 057 (2021), arXiv:2105.10493 [hep-ph].
- [57] A. Azatov, M. Vanvlasselaer, and W. Yin, *JHEP* **10**, 043 (2021), arXiv:2106.14913 [hep-ph].
- [58] I. Baldes, S. Blasi, A. Mariotti, A. Sevrin, and K. Turbang, *Phys. Rev. D* **104**, 115029 (2021), arXiv:2106.15602 [hep-ph].
- [59] A. Azatov, G. Barni, S. Chakraborty, M. Vanvlasselaer, and W. Yin, *JHEP* **10**, 017 (2022), arXiv:2207.02230 [hep-ph].
- [60] A. Azatov and M. Vanvlasselaer, *JCAP* **01**, 058 (2021), arXiv:2010.02590 [hep-ph].
- [61] A. Azatov, M. Vanvlasselaer, and W. Yin, *JHEP* **03**, 288 (2021), arXiv:2101.05721 [hep-ph].
- [62] Y. Hamada, R. Kitano, and W. Yin, *JHEP* **10**, 178 (2018), arXiv:1807.06582 [hep-ph].
- [63] T. Yanagida, *Conf. Proc. C* **7902131**, 95 (1979).
- [64] M. Gell-Mann, P. Ramond, and R. Slansky, *Conf. Proc. C* **790927**, 315 (1979), arXiv:1306.4669 [hep-th].
- [65] S. L. Glashow, *NATO Sci. Ser. B* **61**, 687 (1980).
- [66] R. N. Mohapatra and G. Senjanovic, *Phys. Rev. Lett.* **44**, 912 (1980).
- [67] P. Minkowski, *Phys. Lett. B* **67**, 421 (1977).
- [68] W. Yin, *Phys. Lett. B* **785**, 585 (2018), arXiv:1808.00440 [hep-ph].
- [69] M. Fukugita and T. Yanagida, *Phys. Lett. B* **174**, 45 (1986).
- [70] A. Pilaftsis, *Nucl. Phys. B* **504**, 61 (1997), arXiv:hep-ph/9702393.
- [71] W. Buchmuller and M. Plumacher, *Phys. Lett. B* **431**, 354 (1998), arXiv:hep-ph/9710460.
- [72] E. K. Akhmedov, V. A. Rubakov, and A. Y. Smirnov, *Phys. Rev. Lett.* **81**, 1359 (1998), arXiv:hep-ph/9803255.
- [73] T. Asaka and M. Shaposhnikov, *Phys. Lett. B* **620**, 17 (2005), arXiv:hep-ph/0505013.
- [74] Y. Hamada and R. Kitano, *JHEP* **11**, 010 (2016), arXiv:1609.05028 [hep-ph].
- [75] S. Eijima, R. Kitano, and W. Yin, *JCAP* **03**, 048 (2020), arXiv:1908.11864 [hep-ph].
- [76] D. Besak and D. Bodeker, *JCAP* **03**, 029 (2012), arXiv:1202.1288 [hep-ph].
- [77] P. Hernández, M. Kekic, J. López-Pavón, J. Racker, and J. Salvado, *JHEP* **08**, 157 (2016), arXiv:1606.06719 [hep-ph].

- [78] L. D. Landau and I. Pomeranchuk, Dokl. Akad. Nauk Ser. Fiz. **92**, 535 (1953).
- [79] A. B. Migdal, Phys. Rev. **103**, 1811 (1956).
- [80] S. Chang and K. Choi, Phys. Lett. B **316**, 51 (1993), arXiv:hep-ph/9306216.
- [81] T. Moroi and H. Murayama, Phys. Lett. B **440**, 69 (1998), arXiv:hep-ph/9804291.
- [82] J. H. Chang, R. Essig, and S. D. McDermott, JHEP **09**, 051 (2018), arXiv:1803.00993 [hep-ph].
- [83] N. Bar, K. Blum, and G. D'Amico, Phys. Rev. D **101**, 123025 (2020), arXiv:1907.05020 [hep-ph].
- [84] T. Moroi, K. Mukaida, K. Nakayama, and M. Takimoto, JHEP **11**, 151 (2014), arXiv:1407.7465 [hep-ph].
- [85] K. Nakayama and W. Yin, JHEP **10**, 026 (2021), arXiv:2105.14549 [hep-ph].
- [86] E. Baracchini et al. (PTOLEMY), (2018), arXiv:1808.01892 [physics.ins-det].
- [87] D. McKeen, Phys. Rev. D **100**, 015028 (2019), arXiv:1812.08178 [hep-ph].
- [88] Z. Chacko, P. Du, and M. Geller, Phys. Rev. D **100**, 015050 (2019), arXiv:1812.11154 [hep-ph].